ORIGINAL RESEARCH

An Iron Metabolism-Related *SLC22A17* for the Prognostic Value of Gastric Cancer

Jianming Wei[1],*
Xibo Gao[2],*
Yulan Qin [3]
Tong Liu[1]
Yani Kang [3]

[1]Department of General Surgery, Tianjin Medical University General Hospital, Tianjin 300052, People's Republic of China; [2]Department of Dermatology, Tianjin Children's Hospital, Tianjin 300074, People's Republic of China; [3]School of Biomedical Engineering, Bio-ID Center, Shanghai Jiao Tong University, Shanghai 200240, People's Republic of China

*These authors contributed equally to this work

Purpose: Gastric cancer (GC) is a type of malignant cancer with a poor prognosis. The iron's metabolism plays an important role in the process of GC. The aim of this study was to evaluate the effectiveness of *SLC22A17*, associated with iron metabolism, in predicting the prognosis of GC patients.

Materials and Methods: We analyzed genes related to iron metabolism of gastric cancer mRNA-seq data from TCGA database. We identified an iron metabolism-related *SLC22A17* as an independent prognostic factor using univariate and multivariate Cox regression analysis.

Results: Further research showed that *SLC22A17* was related with many pathways involved in the process of gastric cancer, and the expression was associated with diverse cancer-infiltrating immune cells. The expression of *SLC22A17* was associated with T (Topography).

Conclusion: We validated that *SLC22A17* associated with iron metabolism could serve as a prognostic biomarker for GC patients.

Keywords: gastric cancer, iron metabolism, *SLC22A17*, prognostic marker

Introduction

Gastric cancer (GC) is the fifth most frequently diagnosed cancer and the third leading cause of cancer deaths worldwide.[1] Patients with early gastric cancer (EGC) usually have mild to no symptoms. Notably, the mild symptoms are similar to symptoms of gastritis and gastric ulcer.[2] Surgery is an important treatment method for GC,[3] and there are many other treatment ways for GC, such as chemotherapy, radiotherapy. However, such treatments have not improved the 5-year survival rate of patients at advanced stages.[4] Iron metabolism has a critical role in cancer as cancers generally have a high demand for Fe (III), a nutrient essential for a variety of biochemical processes. High-grade gliomas may be detectable with a radiotracer that targets Fe (III) transport.[5] Additionally, many carcinogenesis-related changes are observed in iron metabolism in lung cancers with chronic obstructive pulmonary disease.[6] Iron metabolism is also altered in hepatic tumors, particularly in liver cancer stem cells (CSC).[7] However, the prognostic value of a gene signature associated with iron metabolism in GC has not been adequately explored.

To assess the potential prognostic value of genes associated with iron metabolism in GC, we performed univariate and multivariate Cox regression analysis and showed that an iron metabolism-related gene *SLC22A17* could serve as a prognostic biomarker for GC patients. We present the following article/case in accordance with the TRIPOD reporting checklist.

Correspondence: Yani Kang
Tel +86-21-3420-7324
Email kangyani@sjtu.edu.cn

Materials and Methods
Data Preprocessing
GC gene expression profiles and clinical factor data were downloaded from the TCGA database. Seventy iron metabolism-related genes, as shown in Supplementary Table 1, were obtained from a previous study.[8] Differentially expressed iron metabolism-related genes with |logFC| >1 and p-value < 0.05 were identified using edgeR from the R software. Following this, differentially expressed iron metabolism-related genes were taken into consideration for the next step of the analysis. The merged mRNA and clinical factor data with *p*-value < 0.05 were selected by performing univariate and multivariate Cox regression. CCLE database (881 samples, Broad Institute, Novartis Institutes for Biomedical Research) was used to evaluate the correlation of *SLC22A17* expression. *FTHL17* and *FTMT* were excluded.

Protein–Protein Interaction Network Construction and Module Analysis
A protein–protein interaction (PPI) network for the 16 DEGs associated with iron metabolism was constructed using the Search Tool for the Retrieval of Interacting Genes/Proteins (STRING) database (https://string-db.org/).[9] The results were visualized using cytoscape software (version 3.6.0). The results were visualized using Cytoscape software (version 3.6.0). The CytoHubba application, a Cytoscape plugin, was used to select the hub genes.[10]

GO and KEGG Functional Enrichment Analysis
Gene ontology (GO) enrichment and Kyoto Encyclopedia of Genes and Genomes (KEGG) pathway analyses were performed using the R language and Perl software. The installed packages included "colorspace", "dose", "clusterProfiler" and "pathview"[11] A *p*-value < 0.05 was considered to be significant.

Tumor Immune Estimation Resource and Gene Set Enrichment Analysis
Tumor immune estimation resource (TIMER, https://cistrome.shinyapps.io/timer/) provides a comprehensive analysis of different immune cell infiltrate genes wherein their association with clinical factors can also be explored.[12] In the present study, the correlation between the expression levels of solute carrier family 22, member 17 (*SLC22A17)*, the infiltration of immune cells, and clinical outcomes were assessed using the online "Gene module" and "Survival module" tools from the TIMER database. TCGA samples were divided into two groups based on the median expression level of *SLC22A17*. Gene Set Enrichment Analysis (GSEA)[13] was performed on the two groups to explore the enrichment pathways of *SLC22A17*. *p*-value <0.05 and false discovery rate (FDR) <0.25 were set as the cut-off criteria.

Clinical Tissue Samples and Immunochemistry
Human tissue microarrays including 40 GC tumor and adjacent non-tumor tissues were collected between May 2018 and May 2019 from Tianjin Medical University General Hospital, China (Supplementary Table 4). Immunochemistry was performed according to previous study.[14] The follow-up time was calculated from the date of surgery to the date of death, or the last known follow-up. All patients had not undergone related anti-tumor therapies before surgery and wrote informed consent. This study was approved by the Hospital Research Ethics Committees of Tianjin Medical University General Hospital. This study complied with the Declaration of Helsinki.

Statistical Analysis
Statistical analysis of gene expression data of GC and adjacent normal samples was performed using unpaired t-tests. Kaplan-Meier survival analysis, univariate and multivariate Cox regression analyses were used to assess the expression levels of differentially expressed iron metabolism-related genes and clinical factors. All statistical analyses were performed with R software, and statistical significance was set at probability values of *p* < 0.05.

Results
Identification of Differentially Expressed Genes Associated with Iron Metabolism
The mRNA expression profiles in GC tissues (n=375) along with the adjacent non-tumor tissues (n=32) were downloaded from the TCGA database. Of the 50752 genes from TCGA expression data, 70 iron metabolism-related genes were selected. Among the iron metabolism-related genes, 6 genes were identified to be downregulated and 10 to be upregulated using the edgeR package. A heat map (Figure 1A) and volcano plot (Figure 1B) of the 16 genes are shown.

Regulatory Network Analysis of Differentially Expressed Genes Associated with Iron Metabolism

Using the online STRING database and Cytoscape software, 16 genes associated with iron metabolism (10 upregulated and 6 downregulated genes) were filtered into the PPI network complex including 16 nodes and 31 edges (Figure 2A). Average degree of the nodes was 3.88, and the PPI enrichment p-value was < 1·0e-16. The top 10 hub genes were identified to be *STEAP2, HPX, BMP6, STEAP1, FAM132B, SLC11A1, HFE2, CYBRD1, HAMP*, and *TFRC* using Cytoscape software cytoHubba (Figure 2B).

Gene Ontology and Kyoto Encyclopedia of Genes and Genomes Pathway Enrichment Analysis

To further elucidate the function of differentially expressed genes, the " clusterProfiler" package was used to perform functional enrichment analysis.[11] GO enrichment analysis results classified gene functions and pathways into three functional groups: 'Biological process' (BP), 'Cell Components' (CC), 'Molecular Function' (MF). For BP, the upregulated iron metabolism-related genes were enriched in the homeostasis of iron transition metal, and cellular iron ions. For CC, the upregulated iron metabolism-related genes were enriched in the endocytic vesicle lumen, endosome membrane, and endosomal part. For MF, the upregulated iron metabolism-related genes were enriched in activities with NAD or NADP as the acceptor, oxidoreductase activity, oxidizing metal ion

activity, and transition metal ion transmembrane transporter activity (Figure 2C). KEGG pathway analysis was used to analyze the most significantly enriched pathways. The iron metabolism-related genes were involved in mineral absorption, TGF-β signaling pathway, and ferroptosis (Figure 2D).

Four Iron Metabolism-Related Genes Were Associated with Overall Survival

This is an example of an equation: To evaluate the relationship between the expression of DEGs associated with iron metabolism and the overall survival of 407 GC patients, we found that four DEGs were associated with overall survival by using a Log rank test and Kaplan-Meier curve. The DEGs included *SLC22A17* (p=0.005482), *BMP6* (p=0.01441), *HAVCR1* (p=0.02669), and STEAP4 (p=0.03264). The relationship between differentially expressed iron metabolism-related genes and overall survival is shown in Figure 3. We found that three common genes *SLC22A17, BMP6* and *HAVCR1* which were DEGs and associated with overall survival (Figure 4A). The expression of *SLC22A17, BMP6* and *HAVCR1* were shown in Figure 4B–D. We selected the most significantly expressed gene *SLC22A17* for further study.

Gene Set Enrichment Analysis of *SLC22A17*

To explore the molecular functions of *SLC22A17*, we examined the gene expression profiles by GSEA analysis. The results are shown in Figure 5. The top 6 pathways were neuroactive ligand–receptor interaction, calcium
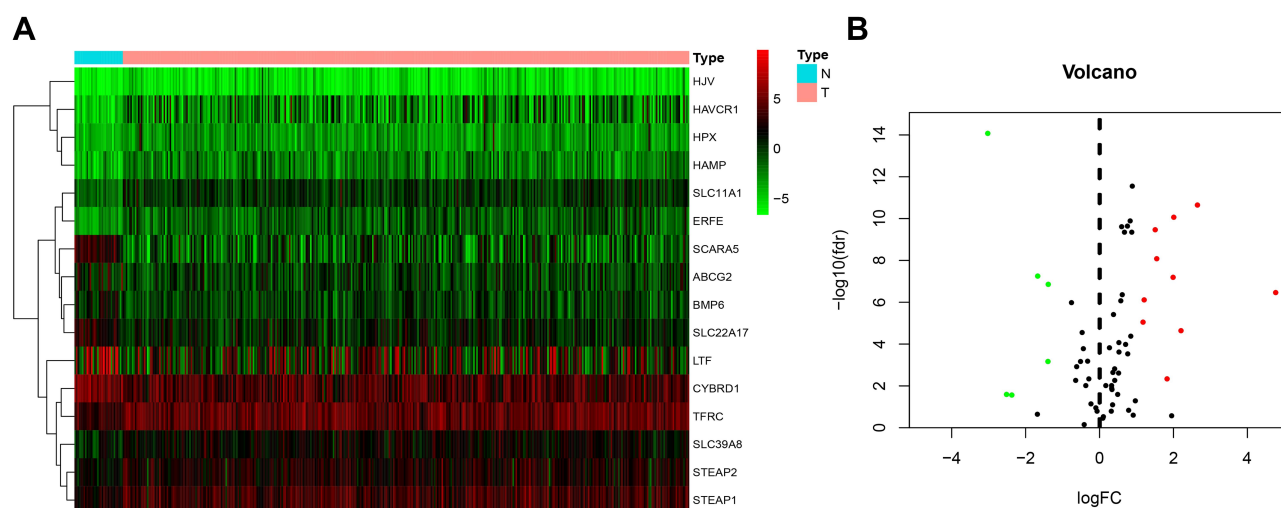

Figure 1 Identification of differentially expressed iron metabolism-related genes. (**A**) Heat map. (**B**) volcano plot of 16 differentially expressed iron metabolism-related genes in GC. Red represents upregulation and green represents downregulation.
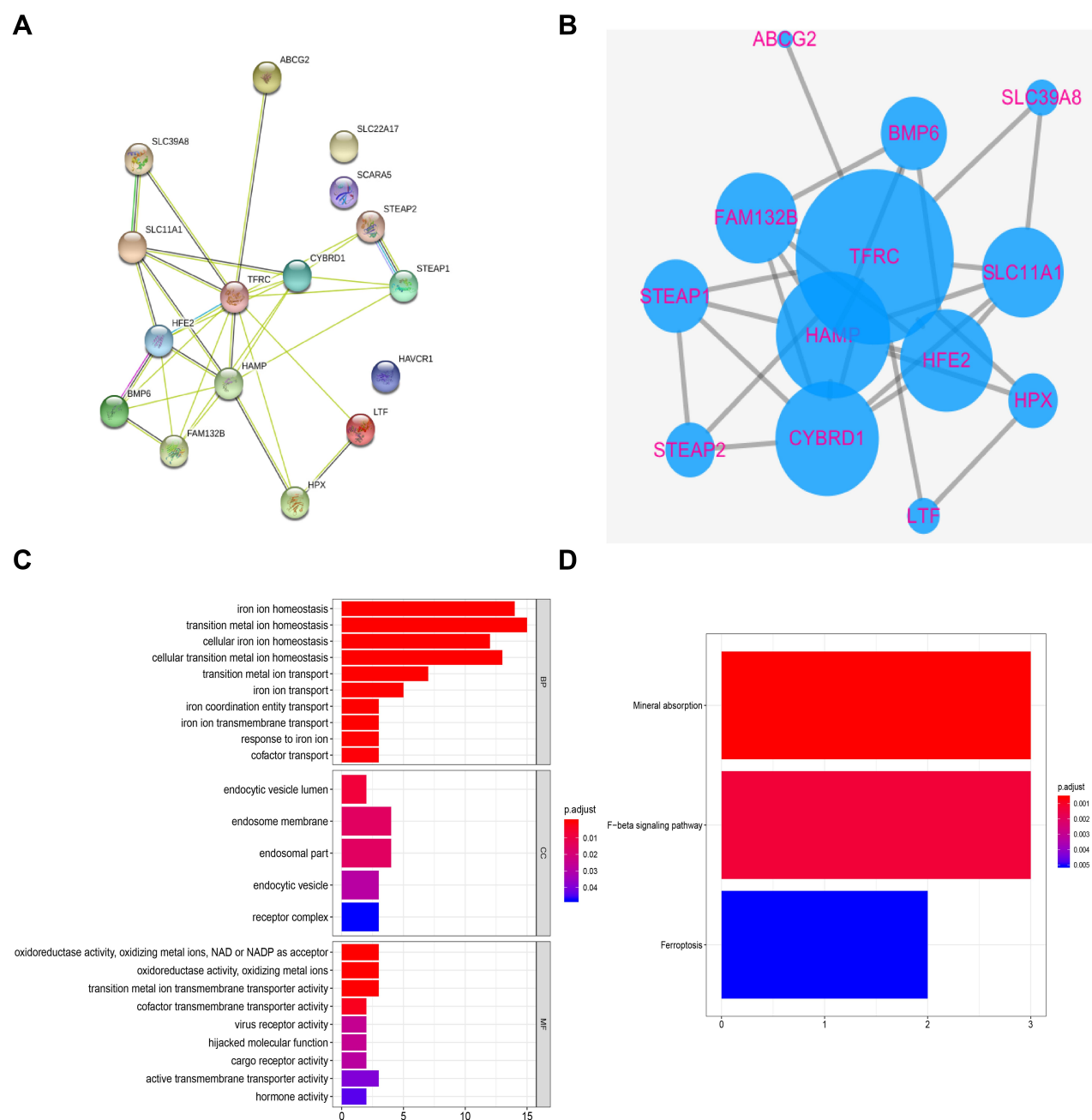
Figure 2 PPI network construction and enrichment analysis of different expressed iron metabolism-related genes. (**A**) A protein–protein interaction network was constructed from the STRING database online. (**B**) The hub genes were screened with cytoHubba. (**C**) Bar plot of GO enrichment in cellular component terms, biological process terms, and molecular function terms. (**D**) Bar plot of KEGG enriched terms.

signaling pathway, vascular smooth muscle contraction, hypertrophic cardiomyopathy, dilated cardiomyopathy, and ECM–receptor interaction.

Correlation of Immune Cell Infiltration with *SLC22A17*

In our study, we used "Gene module" and "Survival module" to evaluate the relationship of *SLC22A17* expression, immune cell infiltration and clinical factors

from the TIMER database. There was a positive correlation between *SLC22A17* expression and the infiltration of dendritic cells (Cor = 0.3, p = 3.53e−09; Figure 6A), neutrophils (Cor = 0.117, p = 2.4e −02; Figure 6B), CD8+ T cells (Cor = 0.116, p = 2.6e−02; Figure 6C), B cell (Cor =0.1051, p = 4.36e −02; Figure 6D), macrophages (Cor = 0.541, p = 1.52e−29; Figure 6E), CD4+ T cells (Cor = 0.475, p = 5.38e−22; Figure 6F)(Table 1).
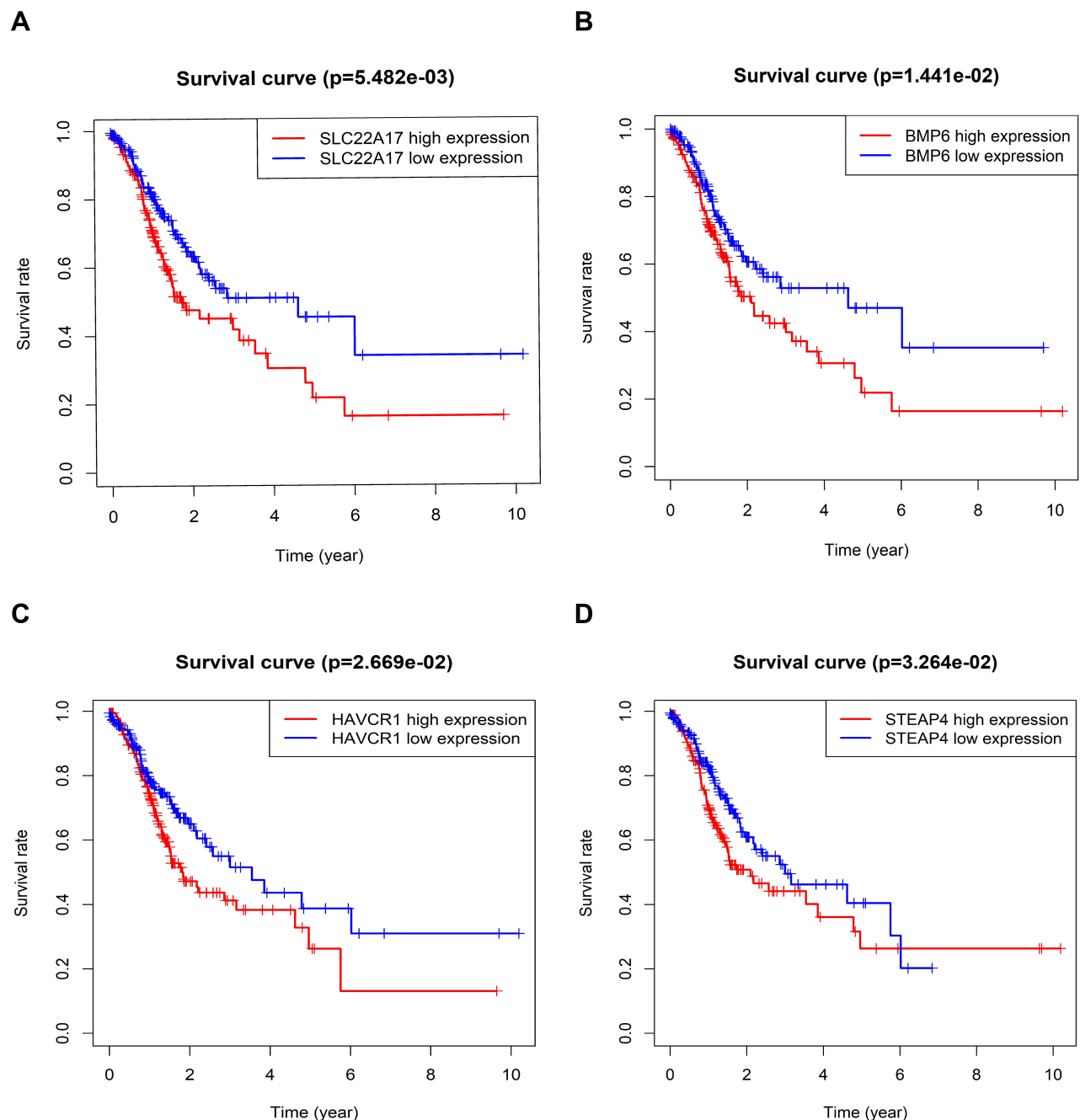
Figure 3 Kaplan Meier survival analysis of all patients with GC according to four iron metabolism-related genes. (**A**) *SLC22A17*. (**B**) *BMP6*. (**C**) *HAVCR1*. (**D**) *STEAP4*.

SLC22A17 Co-Expressed Genes Analysis

Using the co-expression tool on expression data extracted from the 881 samples of CCLE,[15] 261 differentially co-expressed genes were positively (n = 244) or negatively (n = 17) correlated with *SLC22A17* expression. The result was presented in file Supplementary Table 3.

We observed differentially co-expressed genes of the top 10 genes (*GS1-179L18.1, SLC24A3, WNT6, MUC15, JPH3, ECT2, PLS1, HNRNPF, HMGA1, PCBD1*) (Figure 7A).

Altogether, we evaluated molecular functions of the top 10 genes correlated with *SLC22A17* expression. The result showed that the top 10 genes were involved notably in Golgi lumen, calcium channel activity, calcium ion transmembrane transporter activity, AT DNA binding, calcium: cation antiporter activity, peroxisome proliferator activated receptor binding, DNA-(apurinic or apyrimidinic site) endonuclease activity, sodium ion binding, potassium ion binding, retinoid X receptor binding, potassium ion antiporter activity
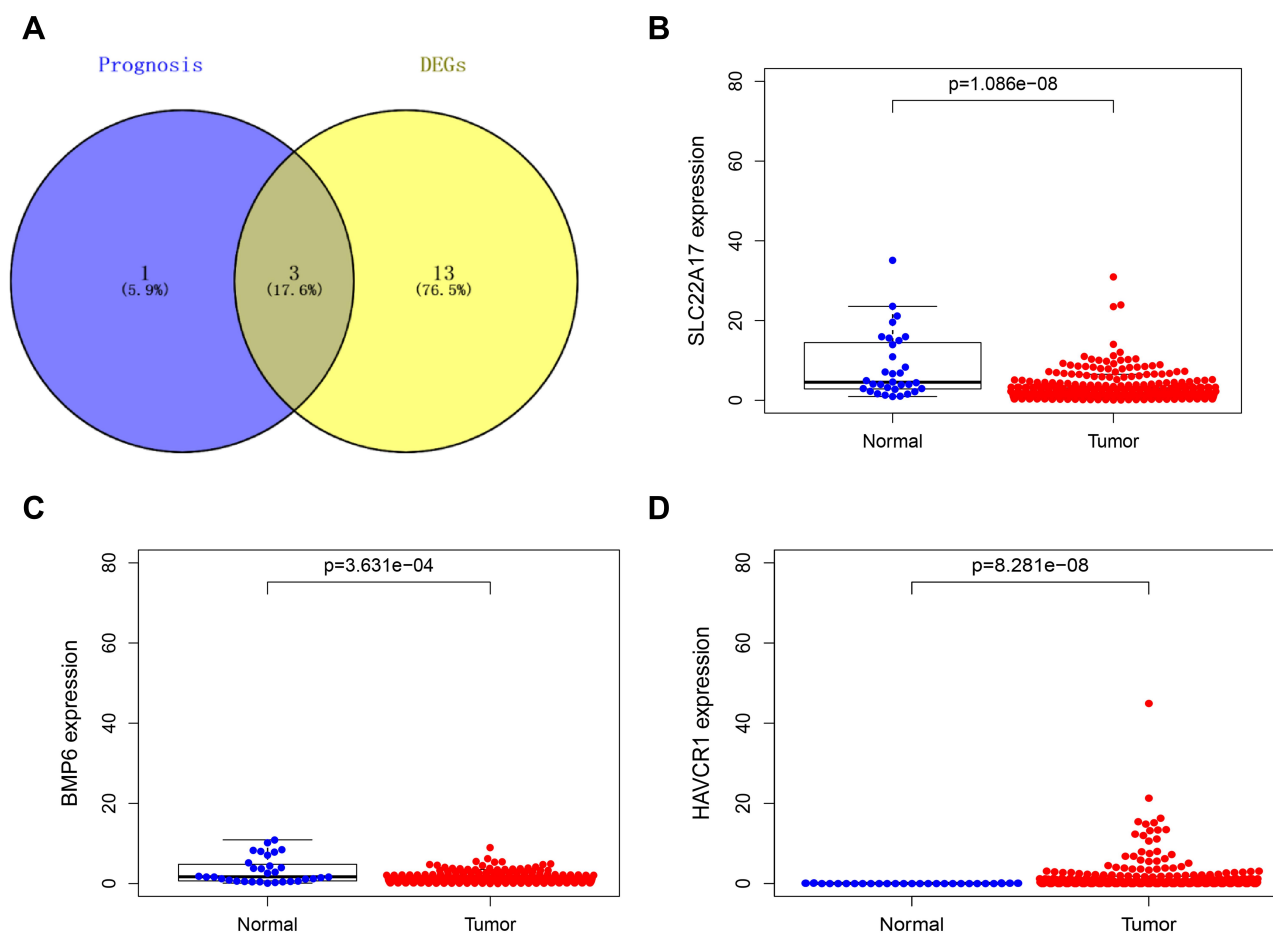
Figure 4 Three common genes expression. (**A**) Three common genes which are DEGs and prognostic genes were identified using VENNY 2.1 online database. (**B**) *SLC22A17*, (**C**) *BMP6* and (**D**) *HAVCR1* were significantly expressed in TCGA database.

(Figure 7B). They were significantly enriched in Folate biosynthesis, Basal cell carcinoma, Melanogenesis, Signaling pathways regulating pluripotency of stem cells, Breast cancer, Gastric cancer, mTOR signaling pathway, Cushing syndrome, Hippo signaling pathway, Wnt signaling pathway, Hepatocellular carcinoma, Proteoglycans in cancer, Human papillomavirus infection, Alzheimer disease (Figure 7C-7E).

Correlation Between *SLC22A17* Expression and Prognosis in GC Patients

SLC22A17 protein levels were evaluated using immunohistochemical staining (IHC) in Figure 8A and B). A H-score was calculated using the following formula: H-score = (percentage of cells of weak intensity x 1) + (percentage of cells of moderate intensity x 2) + (percentage of cells of strong intensity x 3). The maximum H-score would be 300, corresponding to 100% of cells with strong intensity.[16] The relationship between *SLC22A17* expression and clinical follow-up information

was evaluated by Kaplan-Meier analysis and Log rank test. *SLC22A17* was differentially overexpressed in 40 cases GC samples and adjacent non-tumor tissues (Figure 8C). As shown in Figure 8D, high *SLC22A17* expression was associated with poor overall survival ($p < 0.05$). The relationship of *SLC22A17* expression with clinicopathologic factors was in Table 2. Univariate and multivariate Cox hazard regression analysis were performed to assess the value of these signatures including age, gender, grade, stage, T, N, M and *SLC22A17* expression. We confirmed gender and *SLC22A17* expression as independent predictors of the overall survival in patients with GC (Supplementary Table 2).

Discussion

GC has a high morbidity and mortality rate[17] In GC patients, peritoneal dissemination is an aggravated type of metastasis in gastric cancer.[18] Prognostic biomarkers
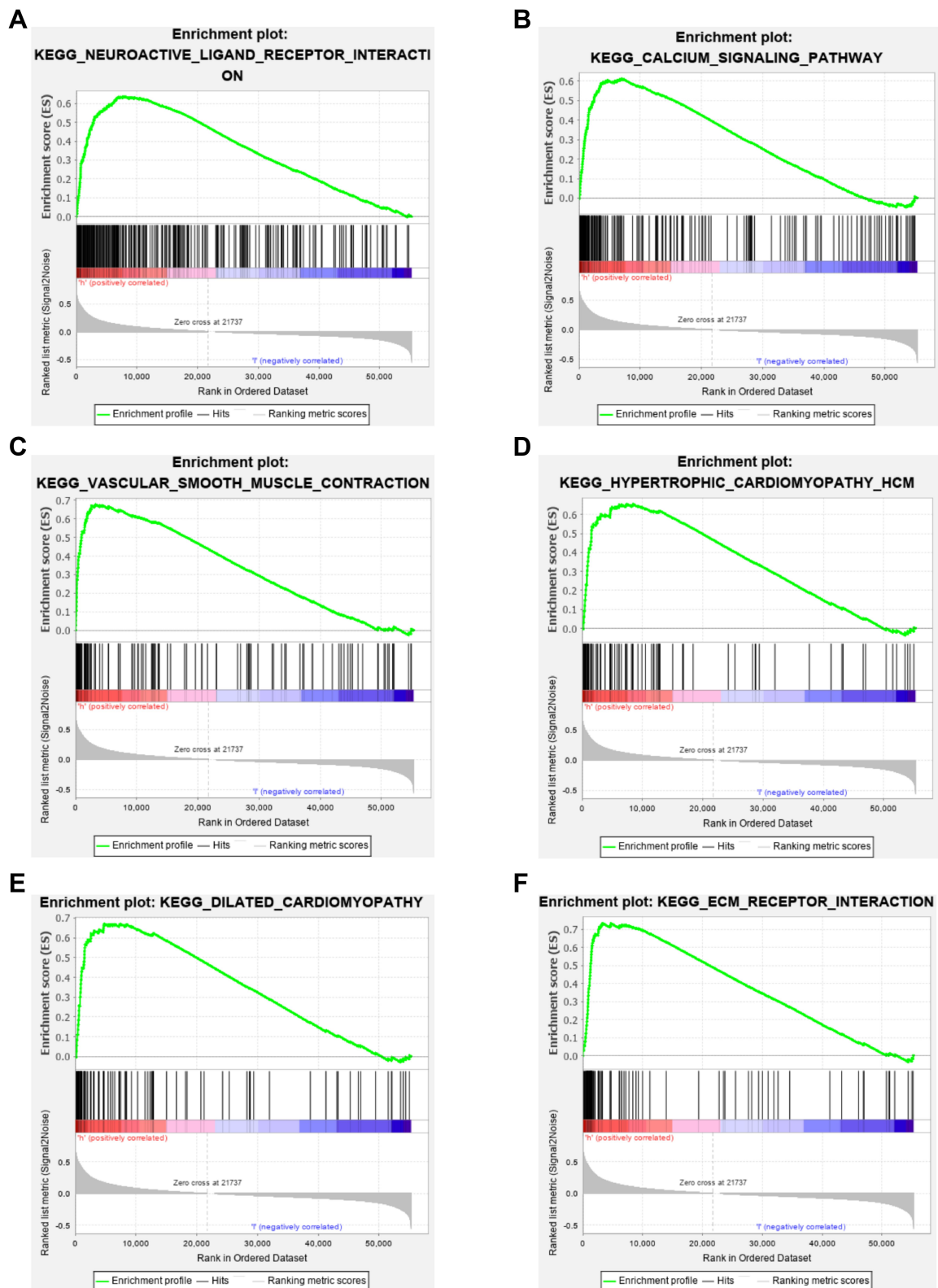
Figure 5 GSEA results of different expression level of *SLC22A17*. Gene set enrichment plots of (**A**) neuroactive ligand–receptor interaction, (**B**) calcium signaling pathway, (**C**) vascular smooth muscle contraction, (**D**) hypertrophic cardiomyopathy HCM, (**E**) dilated cardiomyopathy and (**F**) ECM–receptor interaction.
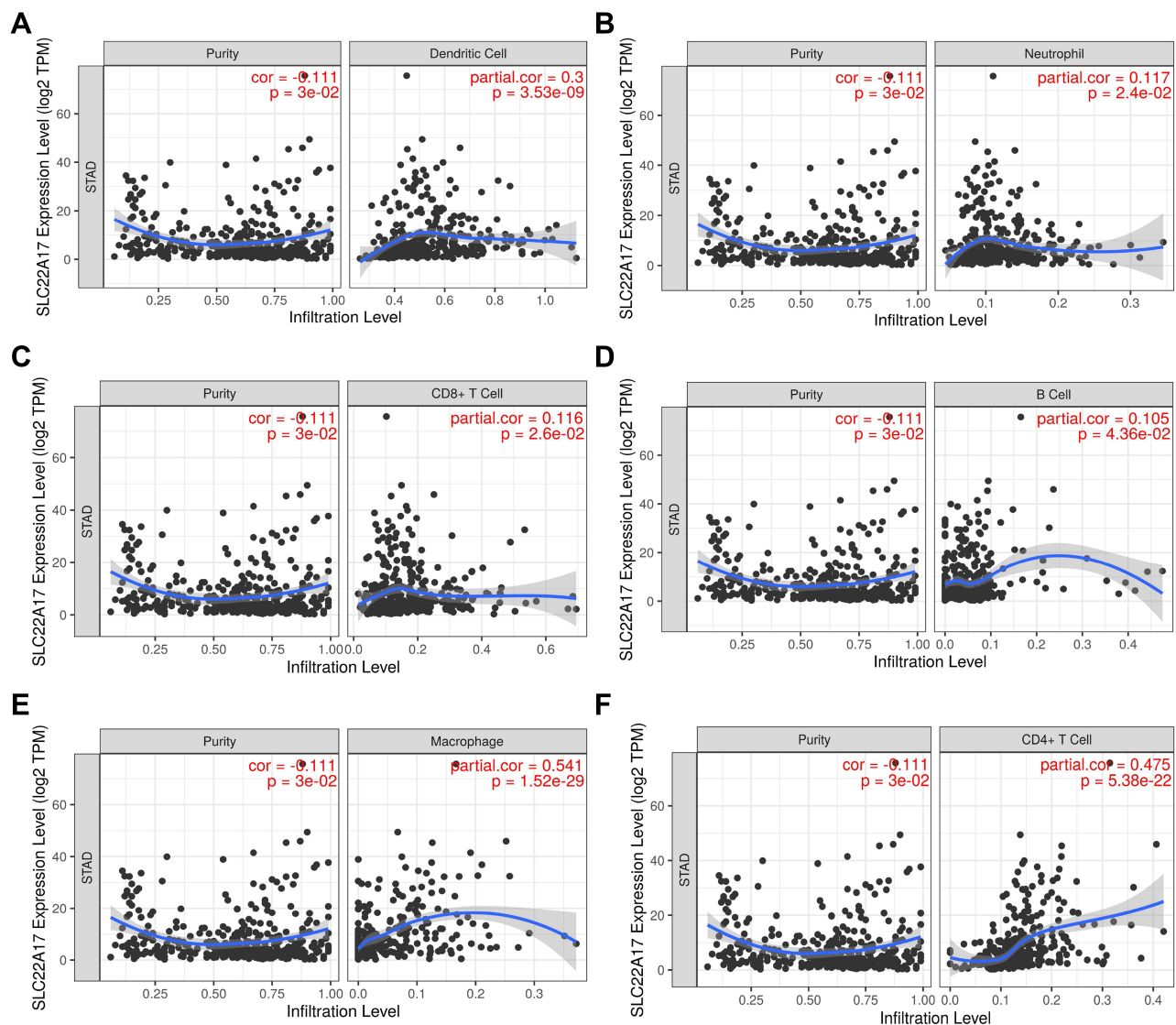
Figure 6 The correlation between different expressed *SLC22A17* and immune cell infiltration (TIMER). The correlation between the expression of *SLC22A17* and the infiltration of (**A**) dendritic cells, (**B**) neutrophils, (**C**) CD8+ T cells, (**D**) B cells, (**E**) macrophages, (**F**) CD4+ T cells.

are critical for GC patients to improve the poor clinical outcomes. This need us to explore novel therapeutic strategies. Prognostic biomarkers are critical for GC patients to improve the poor clinical outcomes. Hence, there is a need to explore novel therapeutic strategies.

Iron is essential for cell growth and proliferation, promoting the production of toxic-free radical species. This has made it a desirable target for cancer treatment and prevention.[19] Previous studies have shown that iron metabolism may contribute to certain cancers, including lung

Table 1 The Cox Proportional Hazard Model of *SLC22A17* Expression, Six Tumor-Infiltrating Immune Cells in GC (TIMER)

	Coefficient	Hazard Ratio	95% CI_l	95% CI_u	*p*-value	Significance
B_cell	5.111	165.775	1.137	24,178.770	0.044	*
CD8_Tcell	−0.829	0.437	0.019	10.091	0.605	n.s
CD4_Tcell	−5.315	0.005	0.000	1.782	0.077	n.s
Macrophage	6.959	1052.183	14.373	77,025.409	0.001	**
Neutrophil	−2.034	0.131	0.000	268.784	0.601	n.s
Dendritic	0.890	2.436	0.123	48.429	0.559	n.s

Notes: Statistical significance was described as follows: n.s, not significant; *$p \leq 0.05$; **$p \leq 0.01$.
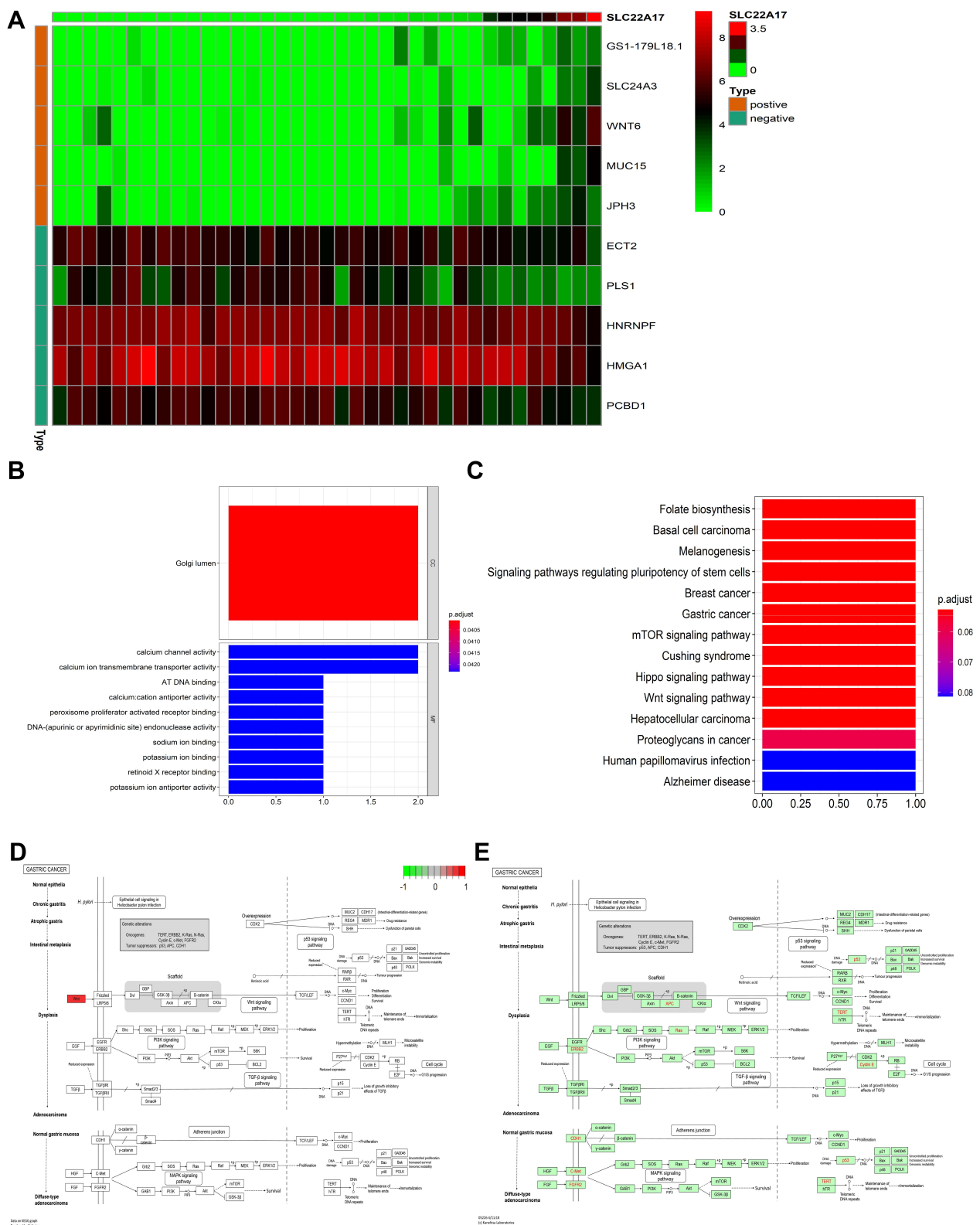
Figure 7 Co-expression of *SLC22A17* analysis. (**A**) Heatmap of the top 10 genes correlated with *SLC22A17* in GC from CCLE database. (**B**) GO and (**C**), (**D**), (**E**) KEGG pathway analyses of the top 10 genes correlated with *SLC22A17*.
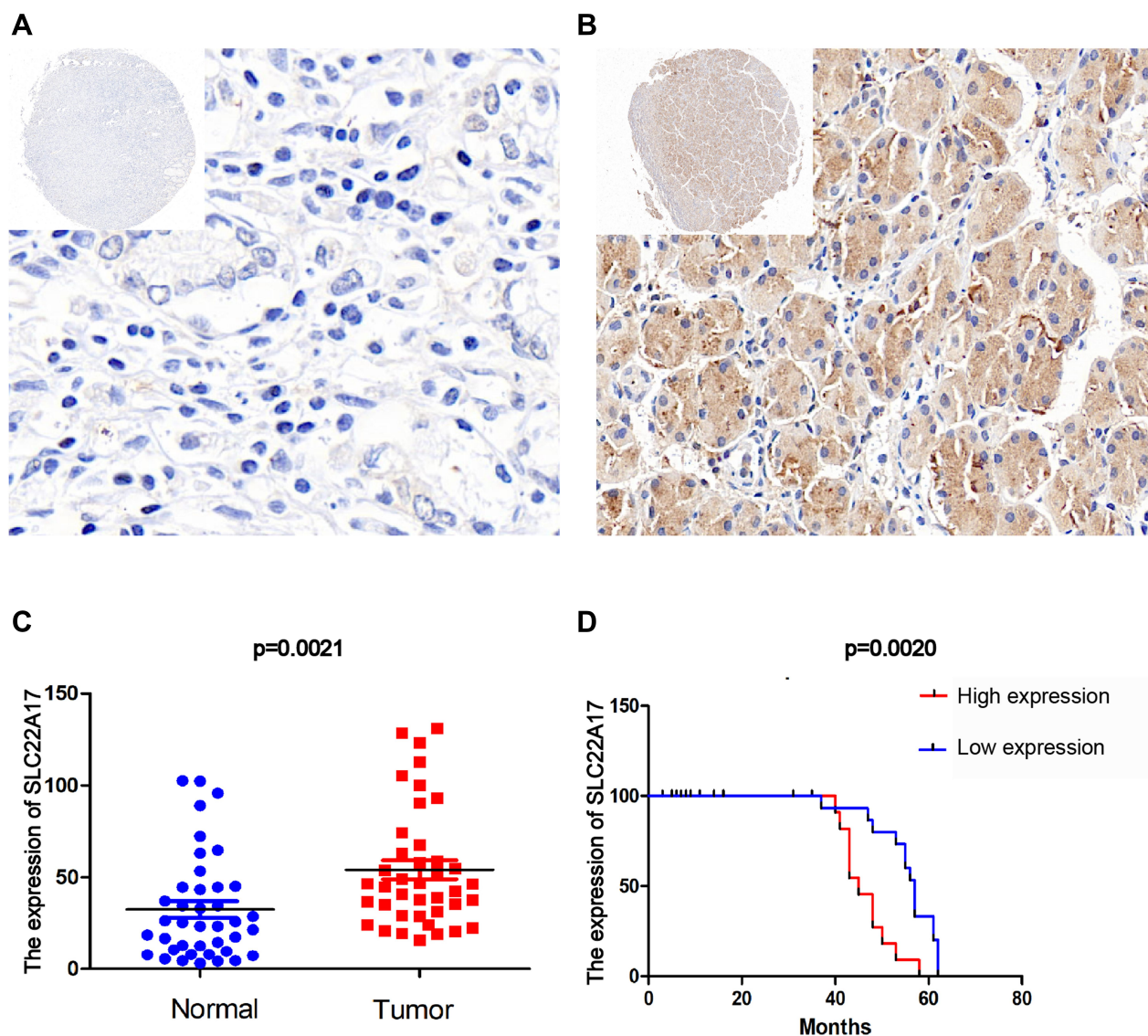
Figure 8 *SLC22A17* expression with prognosis in GC tissue samples. (**A**) negative and (**B**) positive *SLC22A17* expression in GC tissue samples. (**C**) *SLC22A17* was significantly upregulated in our GC samples. (**D**) *SLC22A17* expression is correlated with overall survival rate in GC patients. Kaplan-Meier survival curves show high expression level of *SLC22A17* was significantly correlated with better survival of GC. P-values were calculated by Log rank test.

cancer,[20] leukemia,[21] prostate cancer,[22] and kidney cancer.[23] However, the prognostic signature of iron metabolism in GC needs to be adequately explored.

In this study, we systematically analysed iron metabolism-related genes using the TCGA gene expression data. The upregulated iron metabolism-related genes were found to be: *SLC39A8, STEAP2, TFRC, STEAP1, HJV, HAMP, SLC11A1, HPX, ERFE, and HAVCR1.* The 6 downregulated iron metabolism-related genes were *SCARA5, LTF, ABCG2, SLC22A17, BMP6,* and *CYBRD1.* To assess the interplay of iron metabolism-related genes, the STRING online database and Cytoscape software were used to construct a PPI network complex that included 16 nodes

and 31 edges. The 10 nodes with the highest degree were *STEAP2, HPX, BMP6, STEAP1, FAM132B, SLC11A1, HFE2, CYBRD1, HAMP,* and *TFRC.* KEGG pathway analysis showed that the three important pathways were mineral absorption, TGF-β signaling pathway, and ferroptosis. Increasing evidence suggests that iron metabolism-related genes play an important role in ferroptosis,[24,25] and related to cell apoptosis and aging.[26,27]

SLC22A17, also referred to as a *neutrophil gelatinase-associated lipocalin receptor* (*NGALR*), was identified as a specific cell surface receptor for *lipocalin 2* (*LCN2*).[28] The expression of *NGAL* and *SLC22A17* are associated with human gliomas,[29] clear cell renal cell carcinoma,[30]

Table 2 Correlations Between *SLC22A17* Expression and Clinicopathologic Features in GC Patients

Clinicopathologic Features	Total 40	Expression of *SLC22A17*		*p* value (χ^2 Test)
		Low	High	
Age				0.746
≥60	27	11/27	16/27	
<60	13	6/13	7/13	
Gender				0.629
Female	11	4/11	7/11	
Male	29	13/29	16/29	
Grade				0.983
2	7	3/7	4/7	
3	33	14/33	19/33	
Stage				0.804
1,2	15	6/15	9/15	
3,4	25	11/25	14/25	
T				0.0224*
1,2	6	0/6	6/6	
3,4	17	17/34	17/34	
N				0.275
0	11	6/11	5/11	
1	4	0/4	4/4	
2	10	5/10	5/10	
3	15	6/15	9/15	
M				NA
M0	40	17/40	23/40	
M1	0			

Notes: Statistical significance was described as follows: NA, not applicable; *$p \leq 0.05$.

pancreatic ductal adenocarcinoma,[31] esophageal carcinoma cells,[32] and esophageal squamous cell carcinoma.[33] In leptomeningeal metastases, cancer cells within the CSF express the iron-binding protein lipocalin-2 (LCN2) and its receptor SCL22A17.[34] In the present study, high expression of *SLC22A17* was associated with poor overall survival. *SLC22A17* also plays an important role in cell fate and bacterial infections via Wnt/β-catenin signalling pathway in the renal inner medullary collecting duct cells,[29] in anthracycline-induced cardiotoxicity in children,[30] and endometrial carcinoma.[28] However, the mechanism of action of *SLC22A17* in gastric cancer remains unclear.

We explored *SLC22A17* pathway enrichment using the GSEA software, and found that the top 6 pathways were neuroactive ligand–receptor interactions, calcium signalling pathway, vascular smooth muscle contraction, hypertrophic cardiomyopathy, dilated cardiomyopathy, and ECM–receptor interactions. Iron-related gene expression

patterns in GC between ferroptosis and iron metabolism still requires further exploration.

The tumour microenvironment (TME) consisted of various components, including the extracellular matrix, endothelial cells, fibroblasts, lymphocytes, and macrophages.[35] TME plays an important role in GC progression and prognosis. In the present study, we demonstrated that the expression of *SLC22A17* was associated with immune cell infiltration of dendritic cells, neutrophils, CD8+ T cells, B cells, macrophages, and CD4+ T cells. Li et al found that CD4+ and CD8+ T cell expression was a predictive indicator of gastric cancer prognosis.[36] Previous reports showed that the infiltration of macrophages,[37] dendritic cells,[38] neutrophils,[39] neutrophils[40] and B cells[41] is directly associated with tumour invasion and clinical outcomes in gastric cancer.

To explore the correlation of iron metabolism-related *SLC22A17* with genes in CCLE database, we identified 261 genes for which the expression is correlated with *SLC22A17*

expression. These genes were involved in folate biosynthesis, basal cell carcinoma, melanogenesis, signalling pathways regulating pluripotency of stem cells, breast cancer, gastric cancer, mTOR signalling pathway, cushing syndrome, hippo signalling pathway, wnt signalling pathway, hepatocellular carcinoma, proteoglycans in cancer, human papillomavirus infection, Alzheimer disease.

In the present study, *SLC22A17* protein level as analysed by IHC showed that *SLC22A17* expression was over-expression in 75% (30/40) and 25% (10/40) of GC tissues. Importantly, patients with *SLC22A17* overexpression had significantly shorter survival times compared to those with a low level of *SLC22A17* expression. Univariate analysis showed that *SLC22A17* overexpression was significantly associated with prognosis in GC patients. Multivariate analysis indicated that *SLC22A17* expression was an independent risk factor for poor prognosis of GC patients. We validated that *SLC22A17* might be used as a novel prognostic marker for GC patients. Previous research has also shown that *SLC22A17* could be a potential predictor of clinical prognosis in GC using bioinformatics.

Conclusion

In conclusion, this study demonstrated that *SLC22A17* overexpression is associated with poor survival in GC patients, suggesting that this gene signature associated with iron metabolism as a promising biomarker show superior accuracy in predicting prognosis for gastric cancer.

Author Contributions

(I) Conception and design: Yani Kang, Jianming Wei. (II) Administrative support: Yani Kang. (III) Provision of study materials or patients: Yulan Qin, Tong Liu. (IV) Collection and assembly of data: Yulan Qin. (V) Data analysis and interpretation: Jianming Wei, Xibo Gao. (VI) Manuscript writing: All authors. (VII) Final approval of manuscript: All authors. All authors made substantial contributions to conception and design, acquisition of data, or analysis and interpretation of data; took part in drafting the article or revising it critically for important intellectual content; agreed to submit to the current journal; gave final approval of the version to be published; and agree to be accountable for all aspects of the work.

Funding

Disclosure

The authors declare that they have no conflicts of interest for this work.

References

1. Bray F, Ferlay J, Soerjomataram I, Siegel RL, Torre LA, Jemal A. Global cancer statistics 2018: GLOBOCAN estimates of incidence and mortality worldwide for 36 cancers in 185 countries. *CA Cancer J Clin*. 2018;68(6):394–424. doi:10.3322/caac.21492
2. Digklia A, Wagner AD. Advanced gastric cancer: current treatment landscape and future perspectives. *World J Gastroenterol*. 2016;22 (8):2403–2414. doi:10.3748/wjg.v22.i8.2403
3. Jin W, Han H, Liu D. Downregulation miR-539 is associated with poor prognosis of gastric cancer patients and aggressive progression of gastric cancer cells. *Cancer Biomark*. 2019;26(2):183–191. doi:10.3233/cbm-190384
4. Oh SC, Sohn BH, Cheong JH, et al. Clinical and genomic landscape of gastric cancer with a mesenchymal phenotype. *Nat Commun*. 2018;9(1):1777. doi:10.1038/s41467-018-04179-8
5. Behr SC, Villanueva-Meyer JE, Li Y, et al. Targeting iron metabolism in high-grade glioma with 68Ga-citrate PET/MR. *JCI Insight*. 2018;3:21. doi:10.1172/jci.insight.93999
6. Brzóska K, Bartłomiejczyk T, Sochanowicz B, et al. Carcinogenesis-related changes in iron metabolism in chronic obstructive pulmonary disease subjects with lung cancer. *Oncol Lett*. 2018;16(5):6831–6837. doi:10.3892/ol.2018.9459
7. Recalcati S, Correnti M, Gammella E, Raggi C, Invernizzi P, Cairo G. Iron Metabolism in Liver Cancer Stem Cells. *Front Oncol*. 2019;9:149. doi:10.3389/fonc.2019.00149
8. Zhang S, Chang W, Wu H, et al. Pan-cancer analysis of iron meta-bolic landscape across the Cancer Genome Atlas. *J Cell Physiol*. 2019. doi:10.1002/jcp.29017
9. Szklarczyk D, Morris JH, Cook H, et al. The STRING database in 2017: quality-controlled protein-protein association networks, made broadly accessible. *Nucleic Acids Res*. 2017;45(D1):D362–d368. doi:10.1093/nar/gkw937
10. Zhang H, Zhong J, Tu Y, et al. Integrated Bioinformatics Analysis Identifies Hub Genes Associated with the Pathogenesis and Prognosis of Esophageal Squamous Cell Carcinoma. *Biomed Res Int*. 2019;2019:2615921. doi:10.1155/2019/2615921
11. Wei J, Wang J, Gao X, Qi F. Identification of differentially expressed circRNAs and a novel hsa_circ_0000144 that promote tumor growth in gastric cancer. *Cancer Cell Int*. 2019;19(1):268. doi:10.1186/s12935-019-0975-y
12. Li T, Fan J, Wang B, et al. TIMER: A Web Server for Comprehensive Analysis of Tumor-Infiltrating Immune Cells. *Cancer Res*. 2017;77 (21):e108–e110. doi:10.1158/0008-5472.Can-17-0307
13. Yang Z, Liang X, Fu Y, et al. Identification of AUNIP as a candidate diagnostic and prognostic biomarker for oral squamous cell carcinoma. *EBioMedicine*. 2019;47:44–57. doi:10.1016/j.ebiom.2019.08.013
14. Cai X, Ding H, Liu Y, et al. Expression of HMGB2 indicates worse survival of patients and is required for the maintenance of Warburg effect in pancreatic cancer. *Acta Biochim Biophys Sin (Shanghai)*. 2017;49(2):119–127. doi:10.1093/abbs/gmw124

15. Barretina J, Caponigro G, Stransky N, et al. The Cancer Cell Line Encyclopedia enables predictive modelling of anticancer drug sensitivity. *Nature*. 2012;483(7391):603–607. doi:10.1038/nature11003

16. Azim HA, Peccatori FA, Brohée S, et al. RANK-ligand (RANKL) expression in young breast cancer patients and during pregnancy. *Breast Cancer Res*. 2015;17(1):24. doi:10.1186/s13058-015-0538-7

17. Allemani C, Weir HK, Carreira H, et al. Global surveillance of cancer survival 1995–2009: analysis of individual data for 25,676,887 patients from 279 population-based registries in 67 countries (CONCORD-2). *Lancet*. 2015;385(9972):977–1010. doi:10.1016/s0140-6736(14)62038-9

18. Yamaguchi T, Fushida S, Yamamoto Y, et al. Tumor-associated macrophages of the M2 phenotype contribute to progression in gastric cancer with peritoneal dissemination. *Gastric Cancer*. 2016;19 (4):1052–1065. doi:10.1007/s10120-015-0579-8

19. Clarke SL, Thompson LR, Dandekar E, Srinivasan A, Montgomery MR. Distinct TP53 Mutation Subtypes Differentially Influence Cellular Iron Metabolism. *Nutrients*. 2019;11(9):9. doi:10.3390/nu11092144

20. Sukiennicki GM, Marciniak W, Muszyńska M, et al. Iron levels, genes involved in iron metabolism and antioxidative processes and lung cancer incidence. *PLoS One*. 2019;14(1):e0208610. doi:10.1371/journal.pone.0208610

21. Tsuma-Kaneko M, Sawanobori M, Kawakami S, et al. Iron removal enhances vitamin C-induced apoptosis and growth inhibition of K-562 leukemic cells. *Sci Rep*. 2018;8(1):17377. doi:10.1038/s41598-018-35730-8

22. Iron VD. Metabolism in Prostate Cancer; From Basic Science to New Therapeutic Strategies. *Front Oncol*. 2018;8:547. doi:10.3389/fonc.2018.00547

23. Linehan WM, Schmidt LS, Crooks DR, et al. The Metabolic Basis of Kidney Cancer. *Cancer Discov*. 2019;9(8):1006–1021. doi:10.1158/2159-8290.Cd-18-1354

24. Brown CW, Amante JJ, Chhoy P, et al. Prominin2 Drives Ferroptosis Resistance by Stimulating Iron Export. *Dev Cell*. 2019;51 (5):575–586. doi:10.1016/j.devcel.2019.10.007

25. Dixon SJ, Lemberg KM, Lamprecht MR, et al. Ferroptosis: an iron-dependent form of nonapoptotic cell death. *Cell*. 2012;149 (5):1060–1072. doi:10.1016/j.cell.2012.03.042

26. Hassannia B, Vandenabeele P, Vanden Berghe T. Targeting Ferroptosis to Iron Out Cancer. *Cancer Cell*. 2019;35(6):830–849. doi:10.1016/j.ccell.2019.04.002

27. Nakamura T, Naguro I, Ichijo H. Iron homeostasis and iron-regulated ROS in cell death, senescence and human diseases. *Biochim Biophys Acta Gen Subj*. 2019;1863(9):1398–1409. doi:10.1016/j.bbagen.2019.06.010

28. Miyamoto T, Kashima H, Yamada Y, et al. Lipocalin 2 Enhances Migration and Resistance against Cisplatin in Endometrial Carcinoma Cells. *PLoS One*. 2016;11(5):e0155220. doi:10.1371/journal.pone.0155220

29. Liu F, Li N, Yang W, Wang R, Yu J, Wang X. The expression analysis of NGAL and NGALR in clear cell renal cell carcinoma. *Gene*. 2018;676:269–278. doi:10.1016/j.gene.2018.08.060

30. Liu MF, Jin T, Shen JH, et al. NGAL and NGALR are frequently overexpressed in human gliomas and are associated with clinical prognosis. *J Neurooncol*. 2011;104(1):119–127. doi:10.1007/s11060-010-0486-0

31. Gomez-Chou SB, Swidnicka-Siergiejko AK, Badi N, et al. Lipocalin-2 Promotes Pancreatic Ductal Adenocarcinoma by Regulating Inflammation in the Tumor Microenvironment. *Cancer Res*. 2017;77(10):2647–2660. doi:10.1158/0008-5472.Can-16-1986

32. Cui L, Xu LY, Shen ZY, et al. NGALR is overexpressed and regulated by hypomethylation in esophageal squamous cell carcinoma. *Clin Cancer Res*. 2008;14(23):7674–7681. doi:10.1158/1078-0432.Ccr-08-0420

33. Fang WK, Xu LY, Lu XF, et al. A novel alternative spliced variant of neutrophil gelatinase-associated lipocalin receptor in oesophageal carcinoma cells. *Biochem J*. 2007;403(2):297–303. doi:10.1042/bj20060836

34. Chi Y, Remsik J, Kiseliovas V, et al. Cancer cells deploy lipocalin-2 to collect limiting iron in leptomeningeal metastasis. *Science*. 2020;369(6501):276–282. doi:10.1126/science.aaz2193

35. Sakamoto S, Kagawa S, Kuwada K, et al. Intraperitoneal cancer-immune microenvironment promotes peritoneal dissemination of gastric cancer. *Oncoimmunology*. 2019;8(12):e1671760. doi:10.1080/2162402x.2019.1671760

36. Li F, Sun Y, Huang J, Xu W, Liu J, Yuan Z. CD4/CD8 + T cells, DC subsets, Foxp3, and IDO expression are predictive indictors of gastric cancer prognosis. *Cancer Med*. 2019;8(17):7330–7344. doi:10.1002/cam4.2596

37. Li W, Zhang X, Wu F, et al. Gastric cancer-derived mesenchymal stromal cells trigger M2 macrophage polarization that promotes metastasis and EMT in gastric cancer. *Cell Death Dis*. 2019;10 (12):918. doi:10.1038/s41419-019-2131-y

38. Huang XM, Liu XS, Lin XK, et al. Role of plasmacytoid dendritic cells and inducible costimulator-positive regulatory T cells in the immunosuppression microenvironment of gastric cancer. *Cancer Sci*. 2014;105(2):150–158. doi:10.1111/cas.12327

39. Wu X, Qu D, Weygant N, Peng J, Houchen CW. Cancer Stem Cell Marker DCLK1 Correlates with Tumorigenic Immune Infiltrates in the Colon and Gastric Adenocarcinoma Microenvironments. *Cancers*. 2020;12(2):2. doi:10.3390/cancers12020274

40. Wang K, Liu J, Li J. IL-35-producing B cells in gastric cancer patients. *Medicine*. 2018;97(19):e0710. doi:10.1097/md.0000000000010710

41. Wang M, Li Z, Peng Y, et al. Identification of immune cells and mRNA associated with prognosis of gastric cancer. *BMC Cancer*. 2020;20(1):206. doi:10.1186/s12885-020-6702-1